Available online at www.sciencedirect.com
ScienceDirect
Trans. Nonferrous Met. Soc. China 30(2020) 212−222
Transactions of Nonferrous Metals Society of China
www.tnmsc.cn

Preparation and characterization of Martian soil simulant NEU Mars-1

Jin-zhao GUAN[1], Ai-min LIU[1], Kai-yu XIE[1], Zhong-ning SHI[2], Blanka KUBIKOVA[3]

1. Key Laboratory for Ecological Metallurgy of Multimetallic Mineral (Ministry of Education), Northeastern University, Shenyang 110819, China;
2. State Key Laboratory of Rolling and Automation, Northeastern University, Shenyang 110819, China;
3. Institute of Inorganic Chemistry, Slovak Academy of Sciences, Bratislava 84536, Slovakia

Received 8 March 2019; accepted 18 September 2019

Abstract: To develop Martian soil simulant, basalts of the Chahar volcanic group in Wulanchabu, Inner Mongolia, China were selected as the simulant initial materials, which were ground and sorted to a predetermined particle size ratio, and small amounts of magnetite and hematite were added. The main phases of NEU Mars-1 simulant were plagioclase, augite and olivine. The glass transition and crystallization temperatures of NEU Mars-1 were 547.8 and 795.7 °C, respectively. The complex dielectric constant, magnetic conductivity (0.99−1.045), and dielectric loss tangent angles (0.0025−0.030) of NEU Mars-1 were all stable in the frequency range of 2−18 GHz. Mossbauer spectroscopy results showed that the mass ratio of Fe^{2+} to Fe^{3+} in the simulant was 77.6:22.4. The NEU Mars-1 Martian soil simulant demonstrated particle size ratio, chemical composition, phase composition, thermal stability, and dielectric property similar to Martian soil, and can be used as the substitute material to extract oxygen and metals with in-situ resource utilization technologies.

Key words: Martian soil; stimulant; volcanic rock; basalt; in-situ resource utilization

1 Introduction

Expanding humanity's space for survival and utilizing outer space resources are important for the future development of society, economy, science, technology and civilization. Mars is one of the planets in the solar system that are most similar to Earth. It has Earth-like alternating seasons, and a day on Mars is approximately as long as that on Earth [1]. Recent studies indicated that eight erosive scarps were detected on Mars and a substantial amount of water was found [2], suggesting that Mars may have an environment suitable for developing life and providing hope for the future colonization of the planet. Martian soil is mainly formed by physical weathering due to wind and temperature differences, and rock fragmentation caused by meteorite impact [3]. Viking 1, Viking 2, Pathfinder, Spirit, Opportunity, and Curiosity Mars landers have detected and analyzed the chemical composition of Martian soil and found that it is mainly composed of silicon, iron, aluminum, magnesium and calcium. Furthermore, Martian soil is rich in sulfur and chlorine relative to Earth soil [4−10].

Martian soil simulant is a geochemical replica of Martian soil which has similar chemical and mineral composition, particle size, mechanical strength, porosity, density, and electrical property. Soil simulant is an experimental material that is necessary for research regarding Mars landings, agriculture, in-situ utilization of surface resources, and construction. According to the composition

Foundation item: Project (2017YFC0805100) supported by the National Key R&D Program of China; Project (GUIKE AA18118030) supported by Guangxi Innovation-driven Development Program, China; Project (N172502003) supported by the Fundamental Research Funds for the Central Universities, China
Corresponding author: Zhong-ning SHI; Tel: +86-24-83686381; E-mail: znshi@mail.neu.edu.cn
DOI: 10.1016/S1003-6326(19)65193-9

characteristics of Martian soil, similar rocks or synthetic minerals can be found on Earth, and a simulant resembling Martian soil can be developed. It is worth noting that there is a wide range of regolith types on Mars and their chemical and physical compositions differ in different regions. Therefore, the Martian soil simulant can represent the average (chemical and physical compositions), but not the entire planet in detail. To date, publicly reported Martian soil simulants include European Space Agency's ES-X [11], British SSC [12], US JSC Mars-1 [13], MMS [14], MGS-1 [15], acid−alkaline−salt basalt analog soils [16], New Zealand UC Mars-1 [17], South Korea KMS-1 [18], and Chinese JMSS-1 [19].

The ES-X Martian soil simulants were used to carry out ground simulation experiments for rover vehicles. The simulant was focused on the physical and mechanical properties of Martian soil, and its chemical and mineral composition, magnetism, and other properties differed markedly [11]. The SSC series was primarily used to test the passing performance of rover vehicles [12]. JSC Mars-1 Martian soil was used for engineering and simulation experiments. Its initial material was volcanic ash, with a particle size of less than 1 mm, from Mauna Kea, Hawaii. The spectral characteristics of JSC Mars-1 were similar to those of the bright regions of Mars; however, other properties differed markedly from those of Martian soil. As compared to Martian soil (1200−1500 kg/m^3) [20,21], JSC Mars-1 bulk density was relatively low (835 kg/m^3), the abundance of magnetic mineral phases was relatively high (up to 25 wt.%, mainly containing Ti magnetite), and volatile content was high (when being heated to 100 °C, the volatile content was 7.8 wt.%, and when being heated to 600 °C, the volatile content was 21.1 wt.%) [13]. The MMS Martian soil simulant was developed by the Jet Propulsion Laboratory, California Institute of Technology, and it exhibited a low moisture absorption rate. Its initial material, saddleback basalt, was located east of California in the western Mojave Desert. The chemical and mineral composition, physical, mechanical, spectral, and magnetic properties of MMS were similar to those of Martian soil [14]. This simulant has been used in the Phoenix reconnaissance missions, and engineering and related scientific experiments in the Mars Science Laboratory [22,23]. Acid−alkaline−salt basalt analog soils were designed to simulate the dry-deposition of Martian soil onto spacecraft surfaces during an active descent landing scenario with propellant engines [16]. The UC Mars-1 Martian regolith simulant was developed by the University of Canterbury, and it was used as a construction material on Mars [17]. The KMS-1 Martian soil simulant was made into the Mars-crete. Radiation shielding materials were developed through 3D printing equipment using Mars-crete as a raw material to prepare for the establishment of Mars Village [18]. The JMSS-1 Martian soil simulant had chemical and mineral compositions, particle size, and spectral characteristics similar to Martian soil. It can be applied to Mars exploration engineering and laboratory related simulation experiments [19].

This work describes the development and evaluation of a new Martian soil simulant, NEU Mars-1. Based on Mars landing detection data, and referring to the preparation process, chemical composition, and phase composition of JSC Mars-1 and JMSS-1 Martian soil simulants, porous basalt from the Chahar volcanic group in Inner Mongolia was used as the initial material, and small amounts of hematite and magnetite were added to develop a new Martian soil simulant. The simulant was analyzed and characterized according to its particle size, chemical composition, phase, micro-topography, thermal stability, dielectric constant, and Mossbauer spectrum.

2 Selection and characterization of initial material

Martian soil is mainly composed of igneous rock-forming minerals (80−85 wt.%) and has a relatively high olivine content [24−29], suggesting that the formation processes of Martian surface soils are mainly physical weathering, supplemented by chemical weathering. In addition, substantial studies have indicated that basalts are distributed widely on the surface of Mars [26,30−32]. Therefore, based on the formation and distribution of Martian soil, earth basalts with a similar mineral composition to Martian surface rocks and meteorites are selected as the initial material for the development of the soil simulant.

Basalts are widely distributed in China in the northeast, north, southwest, southeastern coastal areas, and the Qinghai−Tibet Plateau. By consulting relevant information and field investigations, the basalt of the Chahar volcanic group in Inner Mongolia owns lower TiO_2 and Al_2O_3 contents as well as higher Fe content, compared with the basalt of other areas. In addition, as the Chahar volcanic group is young, the olivine content of its basalt is comparatively high. Basalt in this region was collected for further analysis and treatment.

The mineral and chemical compositions of the collected raw materials were evaluated. Figure 1 shows the mineral composition of Chahar basalt using X-ray diffraction (XRD, MPDDY2094 with Cu K_α radiation of λ=1.5405 Å, PANalytical) and Fig. 2 shows its micromorphology and mineral distribution using scanning electron microscopy (SEM, Ultra ZEISS) and energy dispersive spectroscopy.

The main phases of the basalt were found to be plagioclase [(Ca,Na)(Al,Si)$_2$Si$_2$O$_8$], augite [(Ca,Mg,Fe)(Si,Al)$_2$O$_6$], and olivine [(Mg,Fe)$_2$SiO$_4$]. It is shown that Chahar basalt is basically consistent with the main minerals in Martian surface rocks and Martian meteorites, and similar to the rock-forming minerals in Martian soil [24−29].

X-ray fluorescence (XRF, ZSX 100e, Rigaku Corporation, Tokyo, Japan) spectra showed that the main components of the basalt were SiO_2 (45.06 wt.%), Al_2O_3 (18.98 wt.%), CaO (8.31 wt.%), Fe_2O_3 (11.46 wt.%), Na_2O (6.12 wt.%), K_2O (3.44 wt.%), TiO_2 (2.91 wt.%), MgO (2.28 wt.%), P_2O_5 (0.97 wt.%), and MnO (0.16 wt.%). The chemical composition is close to that of the real Martian soil [4−10].

Therefore, Chahar basalt can be used as an initial material for the development of Martian soil simulant.

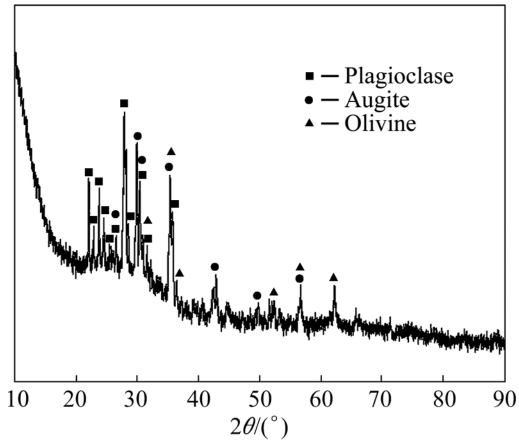

Fig. 1 X-ray diffraction (XRD) patterns of porous basalt (raw material) from Chahar volcanic group, Inner Mongolia

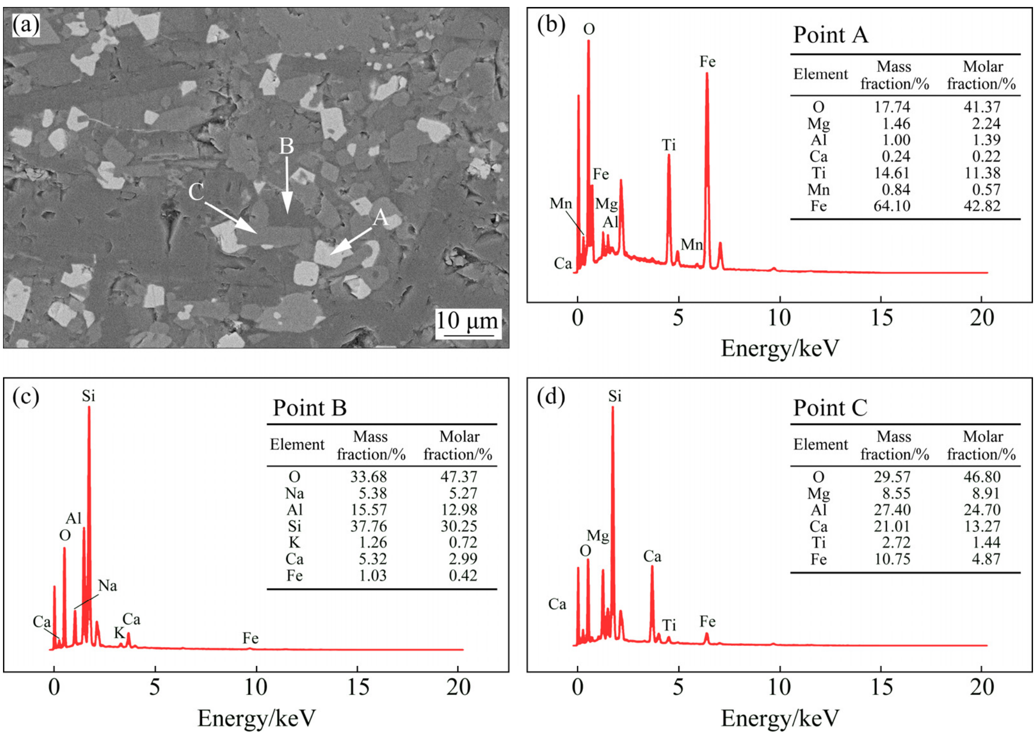

Fig. 2 Back scattered scanning electron microscopy image and energy spectra data of porous basalt (raw material) from Chahar volcanic group, Inner Mongolia

3 Preparation

Collected basalt was cleaned, air-dried, crushed, and ball-milled. Basalt particles were then sieved into six size classifications; above 26 mesh (>680 μm), 60−26 mesh (250−680 μm), 100−60 mesh (150−250 μm), 140−100 mesh (106−100 μm), 200−140 mesh (75−106 μm), and below 200 mesh (<75 μm). The sieved porous basalt powder was baked in a holding oven at (100±5) °C for 12 h to ensure the removal of moisture and possible volatile impurities. According to the gradation curves of JSC Mars-1, MMS, and JMSS-1 Martian soil simulants and in-situ detected particle size of real Martian soil, a reference size ratio for Martian soil was determined (<26 mesh: 15%; 26−60 mesh: 47%; 40−100 mesh: 13%; 100−140 mesh: 7%; 140−200 mesh: 5%; >200 mesh: 13%) following 10 adjustments of the particle size ratio. Granules of the respective particle sizes were then compounded according to the optimum particle size ratio, and after mixing thoroughly, basalt sample particles with the reference particle size composition were obtained.

The Fe content in Martian soil, surface rocks, and meteorites is as high as 16−22 wt.%, and Martian soil also contains Fe and Ti oxides (magnetite and hematite) [25,26,33]. Therefore, it was necessary to add magnetite and hematite to the simulant. Moreover, the particle size ratio of magnetite and hematite was consistent with that of basalt. To ensure that the Fe content of the simulant was 16−22 wt.%, 4 wt.% magnetite and 3 wt.% hematite were added to 93 wt.% of the basalt mixture. The sample was then thoroughly mixed, forming the NEU Mars-1 Martian soil simulant.

4 Characterization of NEU Mars-1

Particle size, elemental and chemical composition, phase, microscopic morphology, thermal stability (DSC-TG), Mossbauer spectroscopy, and dielectric property analyses of the NEU Mars-1 Martian soil simulant were carried out.

4.1 Particle size analysis

The particle size distribution of NEU Mars-1 was analyzed using a Malvern laser particle sizer (Mastersizer 2000 Ver. 5.60) developed by Malvern Instrument Co., Ltd. (UK), as shown in Fig. 3(a). The particle size of the simulant was mainly distributed in 0.1−1200 μm with a few particles less than 100 μm; the median diameter was 247.172 μm. The results of the particle size analysis were used to determine a gradation curve for NEU Mars-1 which was compared with gradation curves of other soil simulants [13,14,19], as shown in Fig. 3(b). The particle size distribution of NEU Mars-1 was generally consistent with that of other Martian soil simulants.

According to Fig. 3(b), the particle size characteristics of JMSS-1, JSC Mars-1, MMS, and NEU Mars-1 could be calculated, as shown in Table 1. The median grain size and the constrained grain size of NEU Mars-1 were similar to those of other Martian soil simulants; however, the nonuniformity coefficient and curvature coefficient were markedly higher.

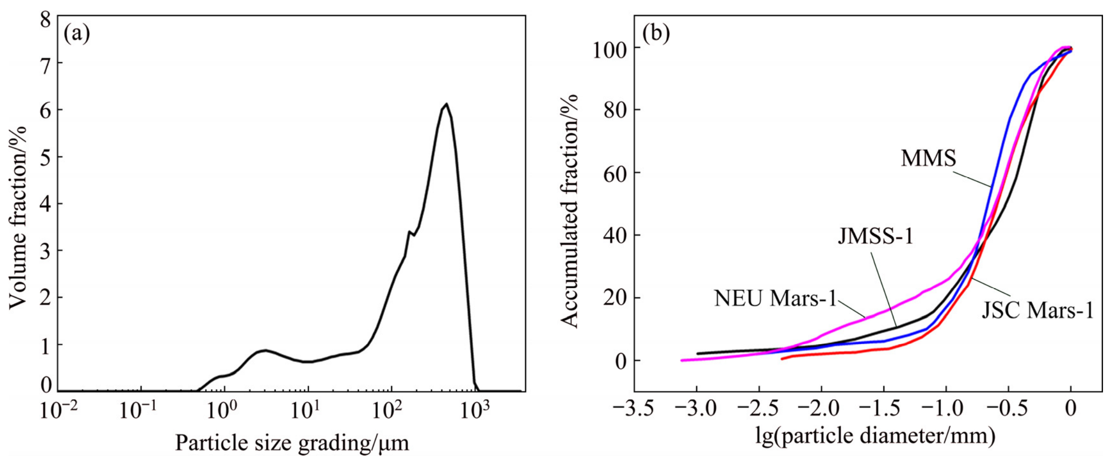

Fig. 3 Particle size distribution of NEU Mars-1 Martian soil stimulant (a) and gradation curve of NEU Mars-1 compared with other Martian soil simulants (b)

4.2 Chemical composition analysis

The chemical composition of NEU Mars-1 was obtained by X-ray fluorescence spectroscopy, which was compared with the composition of Martian soil and JSC Mars-1, MMS, and JMSS-1 simulants, as shown in Table 2. It should be noted that the range of silica content reported is somewhat larger in some Martian soil simulants [7,34]. Compared to Martian soil and other soil simulants, alkali metal oxides (Al_2O_3, Na_2O and K_2O) contents of NEU Mars-1 tended to be high, while the MgO content was found to be low.

4.3 Phase analysis

Phase analysis (Fig. 4) was carried out using X-ray diffraction. The main phases in NEU Mars-1 were found to be plagioclase, augite and olivine. According to the calculation of semi-quantitative analysis of XRD, the phase composition of NEU Mars-1 was plagioclase (47 wt.%), augite (24 wt.%), olivine (15 wt.%), illite (9 wt.%), limonite (3 wt.%) and others (2 wt.%), which was similar to the composition of the real Martian soil detected by Curiosity [26] except that the composition of olivine was relatively lower and that of plagioclase was relatively higher. However, no altered minerals, including sulfates, clay minerals and carbonates were detected in NEU Mars-1; these altered minerals can be added moderately in the future investigation.

4.4 Microscopic morphology

The particle shape of NEU Mars-1 was observed using field emission scanning electron

Table 1 Particle size characteristics of JMSS-1, JSC Mars-1, MMS and NEU Mars-1

Name	Effective grain size, d_{10}/μm	Median grain size, d_{50}/μm	Constrained grain size, d_{60}/μm	Nonuniformity coefficient[1]	Curvature coefficient[2]
JMSS-1	36.1	302.6	374.8	10.4	1.8
JSC Mars-1	79.1	259.2	307.6	3.8	1.2
MMS	69.1	217.6	251.5	3.6	1.4
NEU Mars-1	13.7	247.1	301.9	22.0	4.2

[1] Nonuniformity coefficient $C_u=d_{60}/d_{10}$; [2] Curvature coefficient $C_c=(d_{30})^2/(d_{10}\cdot d_{60})$

Table 2 Chemical compositions of Martian soil and soil simulants (wt.%)

Composition	Martian soil							Martian soil simulant				
	Viking 1 [4]	Viking 2 [4]	Pathfinder [5]	Spirit [6]	Opportunity [7]	Curiosity [8]	Average [9,10]	JSC Mars-1 [14]	MMS [14]	KMS-1 [18]	JMSS-1 [19]	NEU Mars-1
SiO_2	43.00	43.00	42.00	45.80	43.80	42.88	45.41	43.48	49.40	45.40	49.28	43.94
TiO_2	0.66	0.56	0.80	0.81	1.08	1.19	0.91	3.62	1.09	1.80	1.78	2.70
Al_2O_3	7.30	−	10.30	10.00	8.55	9.43	9.71	22.09	17.10	21.86	13.64	17.80
Cr_2O_3	−	−	0.30	0.35	0.46	0.49	0.36	0.03	0.05	0.06	−	−
Fe_2O_3	18.50	17.80	21.70					16.08	10.87		16.00	15.61
FeO				15.80	22.33	19.19*	16.73			12.51*		
MnO	−	−	0.30	0.31	0.36	0.41	0.33	0.26	0.17	0.11	0.14	0.18
MgO	6.00	−	7.30	9.30	7.05	8.69	8.35	4.22	6.08	3.41	6.35	2.13
CaO	5.90	5.70	6.10	6.10	6.67	7.28	6.37	6.05	10.45	9.17	7.56	7.82
Na_2O	−	−	2.80	3.30	1.60	2.72	2.73	2.34	3.28	2.74	2.92	5.58
K_2O	<0.15	<0.15	0.60	0.41	0.44	0.49	0.44	0.70	0.48	2.12	1.02	2.96
P_2O_5	−	−	0.70	0.84	0.83	0.94	0.83	0.78	0.17	0.54	0.30	0.99
SO_3	6.60	8.10	6.00	5.82	5.57	5.45	6.16	0.31	0.10	0.03	−	0.06
Cl	0.70	0.50	0.90	0.53	0.44	0.69	0.68	−	−	−	−	0.07
Total	88.81	75.81	99.80	99.37	99.18	99.85	99.01	99.96	99.24	99.74	98.99	99.84

* The sum of Fe_2O_3 and FeO. For the Viking Landers, Pathfinder soil, JSC Mars−1, MMS, JMSS−1 and NEU Mars−1, total Fe is expressed as Fe_2O_3. For Spirit and Opportunity, average soil total Fe is expressed as FeO [19,35]

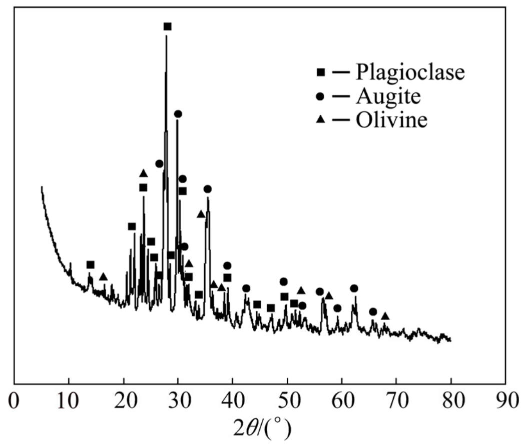

Fig. 4 XRD pattern of NEU Mars-1 Martian soil simulant

microscopy (ZEISS ULTRA PLUS, Germany). Figure 5 shows that NEU Mars-1 simulant consisted of agglomerated large particles (>5 μm), while fine particles (<1 μm) were relatively sparse. Particle shapes tended to be complex because the simulant was obtained by manual crushing and mechanical grinding, resulting in particles with no fixed morphology in granular, block, diamond, and strip forms.

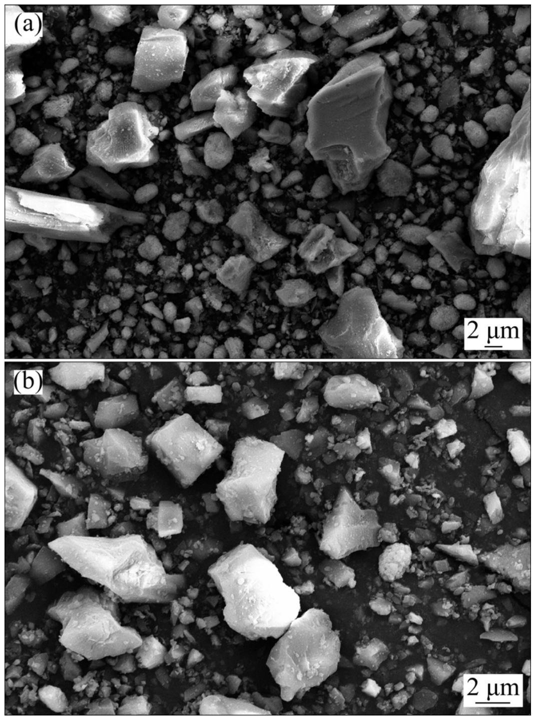

Fig. 5 Particle shape of NEU Mars-1 Martian soil simulant samples

4.5 Thermal stability

To determine the glass transition temperature (T_g), crystallization temperature (T_c), and melting temperature (T_m) of NEU Mars-1, differential scanning calorimetry−thermo-gravimetric analysis (DSC−TG; NETZSCH STA449F3, Germany) was performed [36]. An understanding of thermal stability is important to explore the possibility of using NEU Mars-1 to produce glass products; it can also provide data to support the in-situ utilization of Martian soil to prepare glass. The simulant was heated from room temperature to 1300 °C at a rate of 15 °C/min. Endothermic and exothermic conditions and mass changes were observed, as shown in Figs. 6(a) and (b).

Approximately 1.2% mass attenuation occurred at 100−500 °C, and heat was gradually absorbed due to volatilization and decomposition of impurities such as bound water and ash mixed in the simulant. Above 700 °C, the simulant began to increase in mass (a net gain of approximately 1.0%) as divalent iron-containing minerals began to oxidize. Thermogravimetric analysis shows that the simulant was demonstrated no marked mass

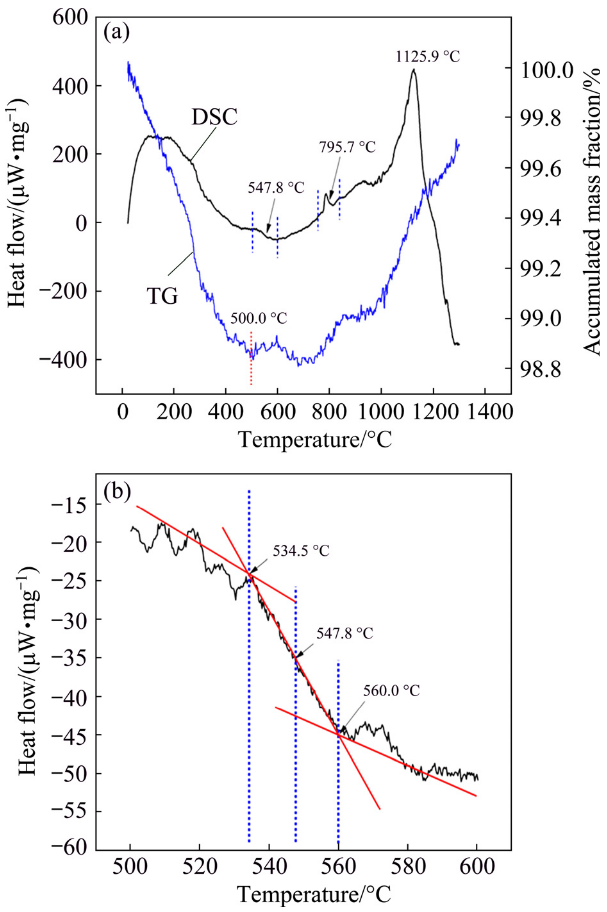

Fig. 6 Results of thermogravimetric analysis (a) and glass transition temperature (b) of NEU Mars-1

increase or loss as the temperature increased. In other words, the simulant contains less water and volatile matter, and exhibits better stability at high temperatures [37].

According to the ASTMD3418 method, T_g (547.8 °C; Fig. 6(b)) was found to be the midpoint between the starting (T_1=534.5 °C) and termination (T_2=560.0 °C) points of the inflectional tangent at the endothermic peak. A second exothermic peak was apparent near 795.7 °C (Fig. 6(a)) corresponding to T_c of the stimulant, indicating the occurrence of a glass phase. Another exothermic peak was apparent at 1125.9 °C, which corresponded to glass recrystallization temperature (T_c').

4.6 Dielectric performance analysis

The dielectric constant of ground materials is generally expressed in the form of a complex dielectric constant. When the ground material is isotropic, it can be expressed by the following equation:

$$\varepsilon_r = \varepsilon' - j\varepsilon'' \tag{1}$$

where ε' is the relative dielectric constant, describing the dispersion characteristics of the dielectric.

For conductive media, the dielectric loss factor ε'' is expressed as

$$\varepsilon'' = \frac{\sigma}{\omega\varepsilon_0} \tag{2}$$

where σ is the dielectric conductivity, ε_0 is the vacuum dielectric constant, and ω is the angular frequency. The dielectric constant of the material is divided into a real ε_r' and an imaginary component ε_r'', and the dielectric loss tangent angle $\tan\delta$ can be obtained from the real and imaginary components of the dielectric constant:

$$\tan\delta = \frac{\varepsilon''}{\varepsilon'} \tag{3}$$

NEU Mars-1 was measured using a microwave network analyzer (N5244A PNA-X, USA) to obtain the complex dielectric constant, magnetic conductivity, and dielectric loss tangent angle, as shown in Fig. 7.

The complex dielectric constant was found to be stable in the 2−18 GHz frequency range (Fig. 7(a)), indicating that the absorbing properties of NEU Mars-1 were weak. The ε'' was almost constant at zero in the test frequency range; hence,

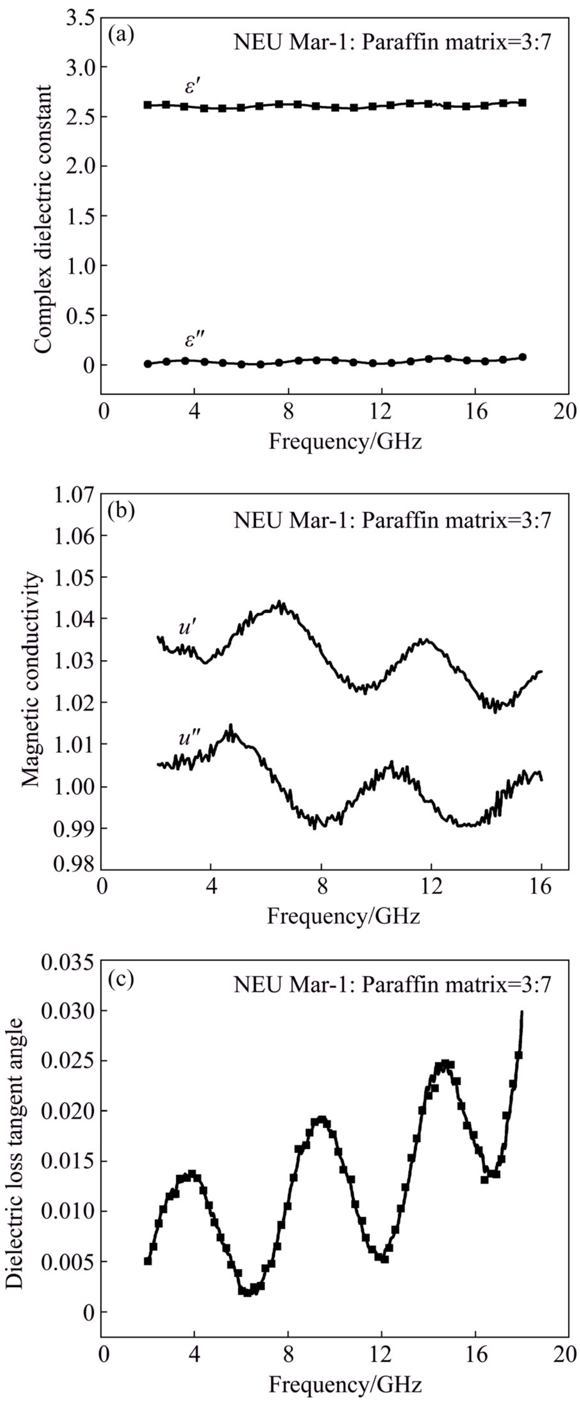

Fig. 7 Complex dielectric constant (a), magnetic conductivity (b) and dielectric loss tangent angle (c) for NEU Mars-1 Martian soil stimulant

the conductivity of NEU Mars-1 was also weak. Figure 7(b) shows that the magnetic conductivity fluctuated (0.99−1.045) in the 2−18 GHz frequency range; however, the magnitude of the change was small, indicating relatively stable magnetic conductivity. Figure 7(c) shows that the dielectric loss tangent angle of NEU Mars-1 fluctuated and increased; however, the variation range (0.0025−

0.030) was almost negligible, indicating no loss of dielectric in 2−18 GHz test frequency range.

4.7 Mossbauer spectrum analysis

Mossbauer spectral analysis of the iron-containing components of NEU Mars-1 is shown in Fig. 8. Three sets of Lorentz spectral references were used to match the Mossbauer spectra, and each reference spectrum was assigned to a corresponding iron ion (Fe^{2+} or Fe^{3+}). The mass ratio of Fe^{2+} to Fe^{3+} in NEU Mars-1 was 77.6:22.4.

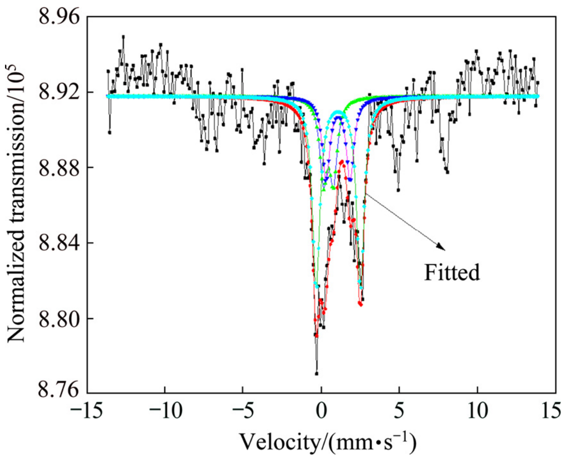

Fig. 8 Mossbauer spectrum of NEU Mars-1 Martian soil stimulant

4.8 Discussion

The particle size distribution of NEU Mars-1 was generally consistent with that of other Martian soil simulants, and the particle size of NEU Mars-1 simulant was mainly distributed in the range of 0.1−1200 μm. However, particle size of real Martian soil is generally distributed in the range from a few microns to 500 μm [38−40], indicating that there is a certain degree of deviation. It should be mentioned that the main application of the NEU Mars-1 simulant is as a feedstock for oxygen and metals extraction using electro-metallurgical methods and the size of the prepared simulant is acceptable for the extraction processes. Compared to Martian soil and other soil simulants, alkali metal oxides (Al_2O_3, Na_2O, and K_2O) contents of NEU Mars-1 tended to be high, while its MgO content was found to be low. The phase composition of NEU Mars-1 was plagioclase (47 wt.%), augite (24 wt.%), olivine (15 wt.%), illite (9 wt.%), limonite (3 wt.%) and others (2 wt.%), which was similar to the composition of real Martian soil detected by Curiosity [26] except that the composition of olivine was relatively lower and that of plagioclase was relatively higher. It was discovered that the Martian soil was composed of 1−7 wt.% magnetic component, the predominant amount of which was magnetite [41−43]. In addition, the hematite was also widely distributed on the Martian surface [44], so magnetite and hematite with a mass ratio of 4 wt.% and 3 wt.%, respectively, were added to the final simulant.

5 Conclusions

(1) Using the basalt of the Chahar volcanic group in Inner Mongolia as the initial material, the NEU Mars-1 Martian soil simulant was developed according to the gradation curves of the Martian soil simulants, JSC Mars-1, MMS, and JMSS-1, and the particle size of Martian soil analyzed in-situ. The initial material was air-dried, crushed, ground, sieved, compounded, mixed, and adjusted to a reference particle size ratio to obtain the simulant.

(2) The results showed that the chemical and phase compositions of the simulant were similar to those of Martian soil. NEU Mars-1 contained relatively high contents of Al_2O_3, Na_2O and K_2O, and low content of MgO. Its main minerals were plagioclase, augite, and olivine.

(3) The T_g and T_c for NEU Mars-1 were 547.8 and 795.7 °C, respectively, and T'_c occurred at 1125.9 °C. The complex dielectric constant, magnetic conductivity (0.99−1.045), and dielectric loss tangent angles (0.0025−0.030) were all stable in the 2−18 GHz frequency range. Mossbauer spectroscopy results showed that the mass ratio of Fe^{2+} to Fe^{3+} was 77.6:22.4. It is concluded that the NEU Mars-1 Martian soil simulant has characteristics similar to real Martian soil and other Martian soil simulants, and can be used for in-situ resource utilization to extract metals and oxygen.

References

[1] HOTAKAINEN M. Mars: From myth and mystery to recent discoveries [M]. Berlin: Springer Science & Business Media, 2010.

[2] DUNDAS C M, BRAMSON A M, OJHA L, WRAY J J, MELLON M T, BYRNE S, MCEWEN A S, PUTZIG N E, VIOLA D, SUTTON S, CLARK E, HOLT J W. Exposed subsurface ice sheets in the Martian mid-latitudes [J]. Science, 2018, 359: 199−201.

[3] GOODING J L, ARVIDSON R, ZOLOTOV M. Physical and chemical weathering [C]//Mars. Tucson: University of Arizona Press, 1992: 626−651.

[4] BANIN A, CLARK B C, WAENKE H. Surface chemistry and mineralogy [C]//Mars. Tucson: University of Arizona Press, 1992: 594−625.

[5] FOLEY C N, ECONOMOU T E, CLAYTON R N, DIETRICH W. Calibration of the Mars Pathfinder alpha proton X-ray spectrometer [J]. Journal of Geophysical Research: Planets, 2003, 108(E12): 8095.

[6] GELLERT R, RIEDER R, ANDERSON R C, BRUCKNER J, CLARK B C, DREIBUS G, ECONOMOU T. KLINGELHOFER G, LUGMAIR G W, MING D W, SQUYRES S W, D'USTON C, WANKE H, YEN A, ZIPFEL J. Chemistry of rocks and soils in Gusev crater from thealpha particle X-ray spectrometer [J]. Science, 2004, 305: 829−832.

[7] RIEDER R, GELLERT R, ANDERSON R C, BRUCKNER J, CLARK B C, DREIBUS G, ECONOMOU T, KLINGELHOFER G, LUGMAIR G W, MING D W, SQUYRES S W, DUSTON C, WANKE H, YEN A, ZIPFEL J. Chemistry of rocks and soils at Meridiani Planum from the alpha particle X-ray spectrometer [J]. Science, 2004, 306: 1746−1749.

[8] BLAKE D F, MORRIS R V, KOCUREK G, MORRISON S M, DOWNS R T, BISH D, MING D W, EDGETT K S, RUBIN D, GOETZ W, MADSEN M B, SULLIVAN R, GELLERT R, CAMPBELL I, TREIMAN A H, MCLENNAN S M, YEN A S, GROTZINGER J, VANIMAN D T, CHIPERA S J, ACHILLES C N, RAMPE E B, SUMNER D, MESLIN P Y, MAURICE S, FORNI O, GASNAULT O, FISK M, SCHMIDT M, MAHAFFY P, LESHIN L A, GLAVIN D, STEELE A, FREISSINET C, NAVARRO- GONZALEZ R, YINGST R A, KAH L C, BRIDGES N, LEWIS K W, BRISTOW T F, FARMER J D, CRISP J A, STOLPER E M, DES MARAIS D J, SARRAZIN P. Curiosity at Gale Crater, Mars: Characterization and analysis of the Rocknest sand shadow [J]. Science, 2013, 341: 1239505.

[9] TAYLOR S R, MCLENNAN S. Planetary crusts: Their composition, origin and evolution [M]. Cambridge: Cambridge University Press, 2009.

[10] MCSWEEN H Y, TAYLOR G J, WYATT M B. Elemental composition of the Martian Crust [J]. Science, 2009, 324: 736−739.

[11] BRUNSKILL C, PATEL N, GOUACHE T P, SCOTT G P, SAAJ C M, MATTHEWS M, CUI Liang. Characterisation of Martian soil simulants for the ExoMars rover testbed [J]. Journal of Terramechanics, 2011, 48: 419−438.

[12] PERKO H A, NELSON J D, GREEN J R. Mars soil mechanical properties and suitability of Mars soil simulants [J]. Journal of Aerospace Engineering, 2006, 19: 169−176.

[13] ALLEN C C, JAGER K M, MORRIS R V, LINDSTROM D J, LINDSTROM M M, LOCKWOOD J P. JSC Mars-1: A Martian soil stimulant [C]//GALLOWAY R G, LOKAJ S. Space 98. Reston, VA: ADS, 1998: 469−476.

[14] PETERS G H, ABBEY W, BEARMAN G H, MUNGAS G S, SMITH J A, ANDERSON R C, DOUGLAS S, BEEGLE L W. Mojave Mars simulant−Characterization of a new geologic Mars analog [J]. Icarus, 2008. 197: 470−479.

[15] CANNON K M, BRITT D T, SMITH T M, FRITSCHE R F, BATCHELDOR D. Mars global simulant MGS-1: A Rocknest-based open standard for basaltic Martian regolith simulants [J]. Icarus, 2019, 317: 470−478.

[16] SCHUERGER A C, GOLDEN D C, MING D W. Biotoxicity of Mars soils: 1. Dry deposition of analog soils on microbial colonies and survival under Martian conditions [J]. Planetary and Space Science, 2012, 72: 91−101.

[17] SCOTT A N, OZE C, TANG Y, O'LOUGHLIN A. Development of a Martian regolith simulant for in-situ resource utilization testing [J]. Acta Astronautica, 2017, 131: 45−49.

[18] LEE T S. In-situ resource utilization (ISRU) construction technology for Moon and Mars [EB/OL]. https://sciences.ucf.edu/class/simulant_ kms1/. 2019−06−16.

[19] ZENG Xiao-jia, LI Xiong-yao, WANG Shi-jie, LI Shi-jie, SPRING N, TANG Hong, LI Yang, FENG Jun-ming. JMSS-1: A new Martian soil stimulant [J]. Earth Planets & Space, 2015, 67: 1−10.

[20] ARVIDSON R, ANDERSON R C, BARTLETT P, BELL J F, CHRISTENSEN P R, CHU P, DAVIS K, EHLMANN B L, GOLOMBEK M P, GOREVAN S, GUINNESS E, HALDEMANN A F C, HERKENHOFF K E, LANDIS G A, LI R, LINDEMANN R, MING D W, MYRICK T, PARKER T J, RICHTER L, SEELOS F P, SODERBLOM L A, SQUYRES S W, SULLIVAN R J, WILSON J. Localization and physical property experiments conducted by Opportunity at Meridiani Planum [J]. Science, 2004, 306: 1730−1733.

[21] ARVIDSON R, ANDERSON R C, BARTLETT P, BELL J F, BLANEY D, CHRISTENSEN P R, CHU P, CRUMPLER L S, DAVIS K, EHLMANN B, FERGASON R, GOLOMBEK M P, GOREVAN S, GRANT J A, GREELEY R, GUINNESS E, HALDEMANN A F C, HERKENHOFF K, JOHNSON J, LANDIS G A, LI R, LINDEMANN R, MCSWEEN H, MING D W, MYRICK T, RICHTER L, SEELOS F P, SQUYRES S W, SULLIVAN R J, WANG Alian, WILSON J. Localization and physical properties experiments conducted by Spirit at Gusev Crater [J]. Science, 2004, 305: 821−824.

[22] KRIECHBAUM K, BROWN K, CADY I, HEYDT M, KLEIN K, KULCZYCHI E, OKON A. Results from testing of two rotary percussive drilling systems [C]//SONG Gang-bing, MALLA R B. Earth and Space 2010: Engineering, Science, Construction, and Operations in Challenging Environments. Honolulu, HI: ASCE, 2010: 1394−1401.

[23] LADINO L A, ABBATT J. Laboratory investigation of Martian water ice cloud formation using dust aerosol simulants [J]. Journal of Geophysical Research: Planets, 2013, 118: 14−25.

[24] CHRISTENSEN P R, RUFF S W, FERGASON R L, KNUDSON A T, ANWAR S, ARVIDSON R E, BANDFIELD J L, BLANEY D L, BUDNEY C, CALVIN W M, GLOTCH T D, GOLOMBEK M P, GORELICK N, GRAFF T G, HAMILTON V E, HAYES A, JOHNSON J R, MCSWEEN H Y, MEHALL G L, MEHALL L K, MOERSCH J E, MORRIS R V, ROGERS A D, SMITH M D, SQUYRES S W, WOLFF M J, WYATT M B. Initial results from the Mini-TES experiment in Gusev Crater from the

Spirit Rover [J]. Science, 2004, 305: 837−842.
[25] MCSWEEN H Y, MCGLYNN I O, ROGERS D. Determining the modal mineralogy of Martian soils [J]. Journal of Geophysical Research: Planets, 2010, 115: 1−10.
[26] BISH D L, BLAKE D F, VANIMAN D T, CHIPERA S J, MORRIS R V, MING D W, TREIMAN A H, SARRAZIN P, MORRISON S M, DOWNS R T, ACHILLES C N, YEN A S, BRISTOW T F, CRISP J A, MOROOKIAN J M, FARMER J D, RAMPE E B, STOLPER E M, SPANOVICH N. X-ray diffraction results from Mars Science Laboratory: Mineralogy of Rocknest at Gale Crater [J]. Science, 2013, 341: 1238932.
[27] CHRISTENSEN P R, RUFF S W, FERGASON R L, KNUDSON A T, ANWAR S, ARVIDSON R E, BANDFIELD J L, BLANEY D L, BUDNEY C, CALVIN W M, GLOTCH T D, GOLOMBEK M P, GORELICK N, GRAFF T G, HAMILTON V E, HAYES A, JOHNSON J R, MCSWEEN H Y, MEHALL G L, MEHALL L K, MOERSCH J E, MORRIS R V, ROGERS A D, SMITH M D, SQUYRES S W, WOLFF M J, WYATT M B. Mineralogy at Meridiani Planum from the Mini-TES experiment on the Opportunity rover [J]. Science, 2004, 306: 1733−1739.
[28] BANDFIELD J L. Global mineral distributions on Mars [J]. Journal of Geophysical Research, 2002, 107: 1−20.
[29] BANDFIELD J L, HAMILTON V E, CHRISTENSEN P R. A global view of Martian surface compositions from MGS-TES [J]. Science, 2000, 287: 1626−1630.
[30] HAMILTON V E, CHRISTENSEN P R. Evidence for extensive, olivine-rich bedrock on Mars [J]. Geology, 2005, 33: 433−436.
[31] MORRIS R V, KLINGELHOFER G, BERNHARDT B, SCHRODER C, RODIONOV D S, SOUZA P A, YEN A, GELLERT R, EVLANOV E N, FOH J, KANKELEIT E, GUTLICH P, MING D W, RENZ F, WDOWIAK T, SQUYRES S W, ARVIDSON R E. Mineralogy at Gusev crater from the Mossbauer spectrometer on the Spirit rover [J]. Science, 2004, 305: 833−836.
[32] MCSWEEN H Y. Martian meteorites as crustal samples [C]//BELL J. The Martian Surface−Composition, Mineralogy, and Physical Properties. Cambridge: Cambridge University Press, 2008: 383−392.
[33] YEN A S, GELLERT R, SCHRODER C, MORRIS R V, BELL J F, KNUDSON A T, CLARK B C, MING D W, CRISP J A, ARVIDSON R E, BLANEY D, BRUCKNER J, CHRISTENSEN P R, DESMARAIS D J, SOUZA P A, ECONOMOU T E, GHOSH A, HAHN B C, HERKENHOFF K E, HASKIN L A, HUROWITZ J A, JOLIFF B L, JOHNSON J R, KLINGELHOFER G, MADSEN M B, MCLENNAN S M, MCSWEEN H Y, RICHTER L, RIEDER R, RODIONOV D, SODERBLOM L, SQUYRES S W, TOSCA N J, WANG Alian, WYATT M, ZIPFEL J. Erratum: An integrated view of the chemistry and mineralogy of Martian soils [J]. Nature, 2005, 436: 49−54.
[34] SQUYRES S W, ARVIDSON R E, RUFF S, GELLERT R, MORRIS R V, MING D W, CRUMPLER L, FARMER J D, MARAIS D J, YEN A, MCLENNAN S M, CALVIN W, BELL J F, CLARK B C, WANG A, MCCOY T J, SCHMIDT M E, SOUZA P A. Detection of silica-rich deposits on Mars [J]. Science, 2008, 320: 1063−1067.
[35] OUYANG Zi-yuan, ZOU Yong-liao. Introduction to Mars science [M]. 2nd ed. Shanghai: Shanghai Science and Technology Education Press, 2017.
[36] WANG Li-peng, ZHANG Tao, ZHANG Lei, WU Ji-si, WANG Yan, ZHOU Ke-chao. Thermostability, mechanical and tribological behaviors of polyimide matrix composites interpenetrated with foamed copper [J]. Transactions of Nonferrous Metals Society of China, 2016, 22: 2336−2346..
[37] LI ping, SUN Da-zhi, WANG Xue, XUE Ke-min, HUA Rui, WU Yu-cheng. Microstructure and thermal stability of sintered pure tungsten processed by multiple direction compression [J]. Transactions of Nonferrous Metals Society of China, 2018, 28: 461−468.
[38] MOORE H J, BICKLER D B, CRISP J A, EISEN H J, GENSLER J A, HALDEMANN A F C, MATIJEVIC J R, REID L K. Soil-like deposits observed by Sojourner, the Pathfinder rover [J]. Journal of Geophysical Research−Planets, 1999, 104: 8729−8746.
[39] CHRISTENSEN P R, MOORE H J. The Martian surface layer [C]//Mars. Tucson: University of Arizona Press, 1992: 686−729.
[40] GOLOMBEK M P, HALDEMANN A F C, SIMPSON R A, FERGASON R L, PUTZIG N E, ARVIDSON R E, BELL J F, MELLON M T. Martian surface properties from joint analysis of orbital, Earth-based, and surface observations [C]//BELL J. The Martian Surface−Composition, Mineralogy, and Physical Properties. Cambridge: Cambridge University Press, 2008: 468−494.
[41] HARGRAVES R B, COLLINSON D W, ARVIDSON R E, SPITZER C R. The Viking magnetic properties experiment: Primary mission results [J]. Journal of Geophysical Research, 1977, 82: 4547−4558.
[42] MADSEN M B, HVIID S F, GUNNLAUGSSON H P, KNUDSEN J M, GOETZ W, PEDERSEN C T, DINESEN A R, MOGENSEN C T, OLSEN M, HARGRAVES R B. The magnetic properties experiments on Mars Pathfinder [J]. Journal of Geophysical Research, 1999, 104: 8761−8780.
[43] BERTELSEN P, GOETZ W, MADSEN M B, KINCH K M, HVIID S F, KNUDSEN J M, GUNNLAUGSSON H P, MERRISON J, NORNBERG P, SQUYRES S W, BELL J F, HERKENHOFF K E, GOREVAN S, YEN A S, MYRICK T, KLINGELHOFER G, RIEDER R, GELLERT R. Magnetic properties experiments on the Mars Exploration Rover Spirit at Gusev Crater [J]. Science, 305: 827−829.
[44] MOORE H J, JAKOSKY B M. Viking landing sites, remote-sensing observations, and physical-properties of Martian surface materials [J]. Icarus, 1989, 81: 164−184.

火星土壤仿真样 NEU Mars-1 的制备及性质表征

管晋钊[1]，刘爱民[1]，谢开钰[1]，石忠宁[2]，Blanka KUBIKOVA[3]

1. 东北大学 多金属共生矿生态化冶金教育部重点实验室，沈阳 110819；
2. 东北大学 轧制技术及连轧自动化国家重点实验室，沈阳 110819；
3. Institute of Inorganic Chemistry, Slovak Academy of Sciences, Bratislava 84536, Slovakia

摘　要：以中国内蒙古乌兰察布市察哈尔火山群的玄武岩为初始原料，并在一定粒度配比的玄武岩中添加少量磁铁矿和赤铁矿，制备 NEU Mars-1 火星土壤仿真样。NEU Mars-1 火星土壤仿真样的主要物相为斜长石、辉石和橄榄石，玻璃转化温度和玻璃结晶温度分别为 547.8 °C 和 795.7 °C。NEU Mars-1 火星土壤仿真样的复介电常数在 2~18 GHz 的频率范围内保持很好的稳定性，介质损耗正切角为 0.0025~0.030，磁导率稳定在 0.99~1.045 范围内。穆斯堡尔谱检测结果表明：NEU Mars-1 火星土壤仿真样中 Fe^{2+}和 Fe^{3+}的质量比为 77.6:22.4。NEU Mars-1 火星土壤仿真样与火星土壤具有类似的粒度配比、化学成分、物相组成、热稳定性和介电性能等特征，可以用于火星资源原位利用提取金属和制备氧气的原料。

关键词：火星土壤；仿真样；火山岩；玄武岩；资源原位利用

(Edited by Bing YANG)